AISTech 2007, Steelmaking Conference Proc., (May 7-10, Indianapolis, IN), AIST, Warrendale, PA, Vol. 1, 2007.

Model of Thermal-Fluid Flow in the Meniscus Region During An Oscillation Cycle

Claudio Ojeda
Labein-Tecnalia
C/Geldo-Parque Tecnologico de Bizkaia- Edificio 700
48160-Derio(Vizcaya)-Spain
Tel.:+34-94-607-3300
Fax:+34-94-607-3349
E-mail:cojeda@labein.es

Brian G. Thomas
University of Illinois at Urbana-Champaign
1206 West Green Street
61801 Urbana (IL)
Tel.:217-333-6919
Fax:217-244-6534
E-mail: bgthomas@uiuc.edu

Jon Barco
Labein-Tecnalia
C/Geldo-Parque Tecnologico de Bizkaia- Edificio 700
48160-Derio(Vizcaya)-Spain
Tel.:+34-94-607-3300
Fax:+34-94-607-3349
E-mail:barco@labein.es

Jose Luis Arana
University of Basque Country
C/Alameda de Urkijo S/N
48013-Bilbao(Vizcaya)-Spain
Fax:+34-94-601-4180
E-mail:jl.arana@ehu.es

Key words: Mold powder, Lubrication, Overflow, Slag rim, Fluid flow, Consumption, Heat flux, Oscillation, Mechanism

INTRODUCTION

In continuous casting of steel, initial solidification and behavior at the meniscus are controlled by many phenomena such as the oscillation stroke and frequency of the mold, flow pattern and velocity field in the molten steel, , the corresponding temperature field and delivery of superheat to the meniscus, top surface level fluctuations, the mold flux behavior and solidified rim formation, and the changes in these behaviors during each oscillation cycle[1, 2]. These meniscus phenomena are important because they control molten slag consumption, lubrication, the formation of oscillation marks, subsurface hooks, and surface defects[3-8]. As an initial step in quantitative understanding of these phenomena, a computational thermal-flow model has been developed to simulate transient behavior in the meniscus region during an oscillation cycle. The flow model includes the evolving velocity fields in both the molten slag and molten steel, the dynamic shape of the steel-slag interface (meniscus) including surface tension forces, the movement and overflow of the steel meniscus, slag consumption into the gap, and the effects of movement of the mold wall and solid slag rim above the meniscus. The coupled heat transfer model predicts temperature and heat flux distributions in the meniscus region and the shape of the solid slag rim, including realistic temperature-dependent properties for the melting and resolidifying slag. The results of this fully mechanistic computational model quantify the fluctuations in the pressure field that in turn greatly affect the flow and consumption of liquid slag, the shape of the meniscus and the formation of oscillation marks. This work helps to illustrate and understand the mechanism of formation of surface defects and quality problems in the cast product so that improvements can be found.

Surface Quality Problems

The majority of surface defects in the continuous casting of steel process originate at, or within the first few millimeters of the meniscus in the mould[9, 10]. Oscillation marks, and the associated subsurface hooks in low carbon steels, can entrap mold powder, inclusions, bubbles, and other impurities that lead to subsequent surface defects. Oscillation marks cause local nonuniformities in heat transfer throughout the mold and are common sites for crack formation.[1, 5] Surface cracks in continuously cast slabs that start at the meniscus include broad-face longitudinal, transverse and star cracks, transverse corner and off corner cracks and narrow face transverse cracks. These are often associated with poor mold powder consumption behavior and uneven mold heat transfer[9]. Whether the initiated surface defects develop into cracks depends on heat transfer and events down the reminder of the mold and below mold exit[11, 12]. New continuous casting mould powders and oscillation cycles are being developed constantly to help improve surface quality, ensure plant safety from breakouts, enable faster casting speeds and meet with tightening environmental constraints. The review of related practices such as mold powder selection to ensure optimum performance[13-16] is a constant concern of continuous-casting operators and quality-control engineers.

Thus, it is important to understand meniscus behavior, slag infiltration into the gap, and how oscillation marks form. Many different possible mechanisms have been proposed for oscillation mark formation. These include: 1), overflow of the liquid steel over the frozen meniscus in the top of the steel shell[1], 2) overflow of the liquid steel over the solidified steel meniscus and remelting of the frozen meniscus[4, 6] 3) bending / unbending of the weak solidified steel shell[17,18]., and 4) thermal stresses in the newly-formed shell [19]. Fundamental understanding of defect formation requires taking into account all the different phenomena that take place at the meniscus, using fundamentally-based computational models of fluid flow, heat transfer, and related phenomena.

Phenomena and Process Description

Phenomena involved in initial solidification and the formation of the oscillation marks include the fluid flow of the steel[1, 17, 21], the corresponding transport of superheat to the meniscus region[12, 22], heat transfer from the steel to the mold walls[23, 24], the melting, fluid flow and resolidification behavior of the mold powder[23], and the motion of the steel / slag interface including surface tension and ferrostatic pressure forces. Of great importance is the effect of the solid slag rim that solidifies against the mold wall on the pressure field and corresponding meniscus behavior[1, 6, 25].

Phenomena related to the slag rim and liquid flux flow and consumption are complex. First the powder is spread over the free surface of the steel on the top of the mold. The powder particles sinter together as they migrate downwards, reject gas bubbles, and melt around carbide particles to form a molten slag layer that floats on top of the molten steel. Some of this molten slag solidifies against the mold wall forming a solid slag rim that moves up and down with the mold wall. Its size depends on powder properties and flow conditions at the meniscus, such as level fluctuations. The oscillation of the mold and the buoyancy of the molten slag cause flow in the region formed between the mold, the flux rim, the steel shell and the steel meniscus. The

infiltration of the slag into the gap between the shell and the mold is caused mainly by the pumping effect created by the oscillation of the mold, and drag by the moving steel shell. It is widely believed that during the negative strip time, the positive pressure generated in the meniscus region pumps molten slag into the gap. On the other hand, during the positive strip time, the increasing distance between the meniscus and the solid slag rim draws molten slag into this region and so consumption correlates with the positive strip time. The rate of flux consumption has a great effect on mold heat transfer, lubrication to prevent sticking of the shell to the mold, and associated surface defects[2, 12].

Objectives

Mathematical models combined together with plant data are key tools to understand meniscus behavior and how oscillation marks and surface defects form. Several previous models have been applied to investigate several of these phenomena independently[3,4,5,12,17,18,22,23,26,30]., including meniscus motion[31] during the oscillation cycle and fluid flow and pressure fluctuations in the gap[5,32]. The objective of this study is to advance quantitative understanding of the meniscus region phenomena by simulating transient fluid flow in the molten slag and molten steel, movement and overflow of the steel-slag interface, slag consumption into the gap, formation of the solid slag rim above the meniscus, and the effects of its movement during the oscillation cycle. A coupled heat transfer model is used to quantify the heat delivered to the mold, the temperature field and the melting / solidifying behavior of the rim.

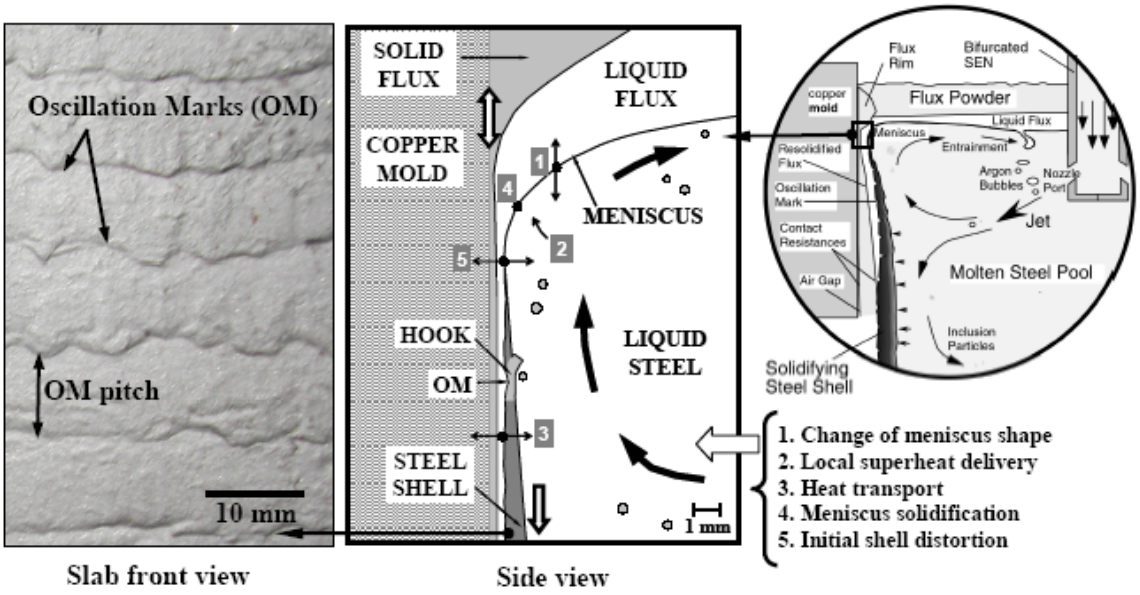

Fig. 1 Description of phenomena in meniscus region[25]

MODEL DESCRIPTION

A computational flow model has been developed to study fluid flow in the meniscus region, the dynamic shape of the steel/slag interface, melting, flow, and resolidification of the mold powder into a solid slag rim, the consumption of slag into the gap between the steel shell and the mold, the evolution of the pressure field and heat transfer to the mold walls, as they all vary with time during an oscillation cycle. A full three-dimensional model is applied to investigate the corner region of the meniscus, and a two-dimensional model is used far from the corner.

The fluid flow model solves the Navier-Stoke's equations, using the Volume of Fluid model to track the air, slag and steel phases and the shape and motion of their interfaces, using the commercial computational fluid dynamics (CFD) package FLUENT. The simulation domain contains powder, liquid slag and molten steel, with the solid / liquid slag layer interface at 1073K and solid steel shell as boundaries, as shown in Fig. 2 and Fig. 3. The gap between the solid slag layer (defined by the 1073 isotherm fixed at the domain wall) and the tip of the solidified steel shell is set at a uniform thickness of 0.5mm , based on calculations using the CON1D model[1] for typical casting conditions. The viscosity and temperature of the liquid slag in the entire domain, including this gap, varies according to the transient calculations, and the temperature-dependent properties of the powder / slag, which are given in Figs. 4 and 5. A wedge-shaped steel shell moving down at the casting

speed in steady-state is assumed, again based on CON1D[1]. The boundaries of the fluid domain are treated as zero-slip walls except the top surface, which is a pressure inlet with a gauge pressure of 0 Pa, the outlet of the gap, which is a pressure outlet (at 0 Pa), and the transverse cuts through the liquid steel, which are given symmetry conditions. Superheat of the molten steel in the region is assumed to be high enough to prevent undercooling and meniscus freezing. The casting conditions and properties are given in Table 1 and Figs. 4 and 5 for the conductivity and viscosity depending on temperature for the slag.

To obtain a reasonable initial condition, the isothermal flow model is first run with no movement in the mold wall and zero casting velocity until the results are unchanged with time, meaning that steady-state has been reached. This requires about 2.0s simulation time. Then the heat flow model is activated with no movement in the wall until a new steady state is reached, which requires around 10 minutes more of simulation time.

The coupled fluid flow and heat flow model calculations are then performed for two oscillation cycles. The heat flow model includes calculation of the heat delivered into the mold, the temperature field and the thickness and shape of solidified slag under time-averaged conditions. In this case, the powder / slag viscosity and conductivity, shown in fig 4 and 5, change according to conditions of melting (heating) or solidification (cooling) [11,23]. At the bottom of the mold side boundary, representing the slag / liquid interface, a temperature boundary condition of 1073K is imposed. At the top of the mold (powder layer), a heat transfer coefficient of 130W/m^{2}K is assumed .The liquidus temperature of the molten steel (1805.9K) is imposed at the liquid slag / molten steel interface, and the solidus temperature (1793.9K) at the cold side of the steel shell tip. The domain, shown by the colored results in Fig. 2, is the same as that for the fluid flow model, except that temperature variations in the molten steel are not calculated.

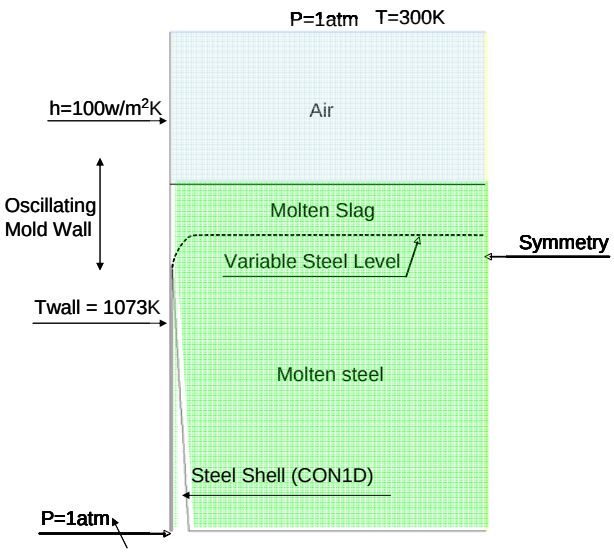

Fig. 2 Model domain (2-D)

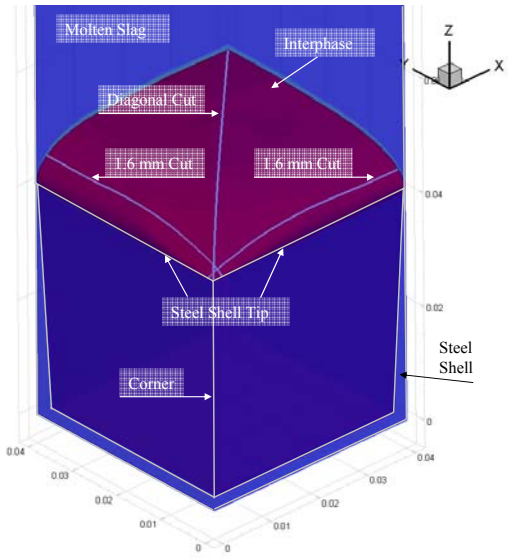

Fig. 3 Model domain (3-D)

Table 1 Operation data used in the simulation

Frequency	155 cpm
Stroke	6.37 mm
Casting velocity	1.42 m/min
Temperature of molten steel	1805.9 K
Density of steel	7000 kg/m3
Viscosity of steel	0.063 Poise
Density of slag	2500 kg/m3
Surface tension molten steel / liquid slag	1.3 N/m

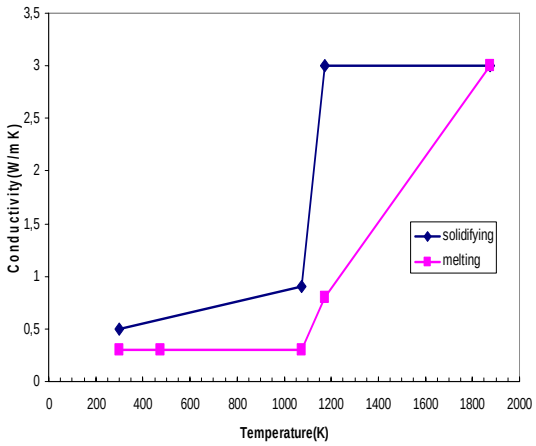

Fig. 4 Conductivity of slag in the model

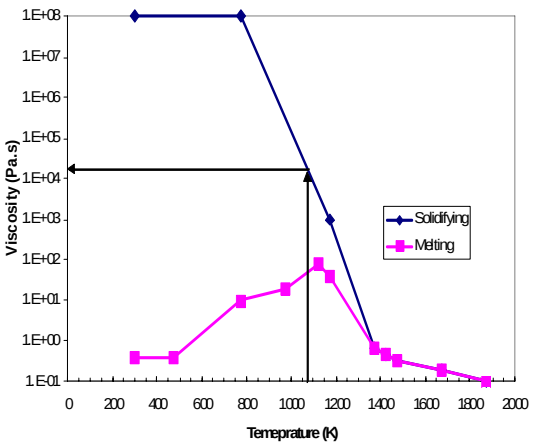

Fig. 5 Viscosity of the slag used in the model

RESULTS

Model Validation

To validate the fluid flow / volume of fluid model, several stationary or "stagnant" cases were run for different molten steel levels above the shell tip. The curved shape of the liquid slag / molten steel interface was computed with the 2D model, for the given slag-steel surface tension (Table 1). This meniscus shape is also calculated using the Bikerman equation[5] Eq. (1). This analytical solution is derived by balancing the pressure forces at each side of the interface and the capillarity forces from surface tension:

$$x = -\sqrt{2a^2 - y^2} + \frac{\sqrt{2a^2}}{2}\ln\left(\frac{\sqrt{2a^2} + \sqrt{2a^2 - y^2}}{y}\right) + 0.3768a \qquad (1)$$

where:

$a^2 = \dfrac{2\sigma}{g(\rho_s - \rho_f)g}$ is the capillary constant

x: distance form the closest point of the interface to the mold
y: vertical distance from the highest point of the interface liquid steel – liquid slag
σ: interfacial tension
ρ_s: density of the steel
ρ_f : density of the liquid mold flux
g: acceleration of gravity

The meniscus shapes from the computational model and Bikerman's equation are compared in Fig. 6. The meniscus shape depends on the head of unsupported liquid (given by the far-field metal level) above the tip of the solidified shell. The comparison shows that the CFD model is able to match the analytical solution exactly, even in the lower part of the Bikerman solution curve, where the unsupported liquid bulges slightly over the edge of the shell tip. This is valid until 12 mm, when the steel overflows over the shell tip, and the equation becomes undefined.

Steady state meniscus shape

The results for the stagnant steady-state 2-D model simulations also illustrate the effect of the liquid level above the shell tip on the shape of the meniscus supported by surface tension. Fig 7 shows the equilibrium (stagnant) interface shape for a range of far-field steel surface levels. For a surface level of 8.7 mm above the shell tip, the interface rises vertically from the shell tip. Increasing liquid level causes the unsupported liquid

steel to bulge over the shell tip. The maximum bulge towards the narrow face of ~1mm occurs at the maximum surface level of 12mm. When the surface level drops below 8.7 mm, the meniscus shape is predicted to remain the same, extending tangentially from the solid shell, so the surface level is predicted to drop below the shell tip. This exposes the hot dendritic interface of the solidifying steel shell to the molten slag, which will cause several problems such as slag entrapment, leading to surface slivers, and thermal stress, leading to deep oscillation marks and associated problems [32, 33].

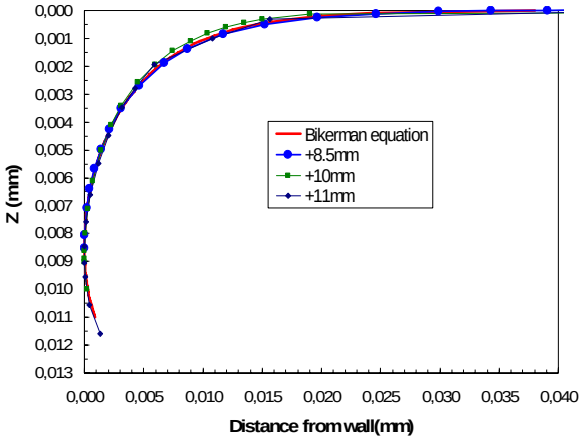

Fig. 6 Computed meniscus shapes compared with analytical solution [5]

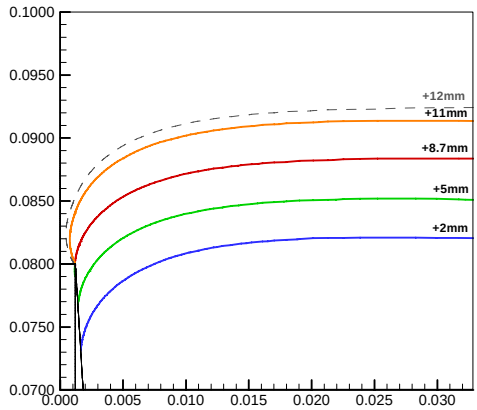

Fig. 7 Interface shapes for different heights of far-field steel surface level

A stagnant simulation is also run with the 3-D model to show the interface shape in the corner region. These results are shown in fig. 8 as cuts at different distances from the mold wall. They show that for cuts closer to the mold wall, the interface has a lower profile than cuts far from the wall, where the shape is coincident with the Bikerman equation.

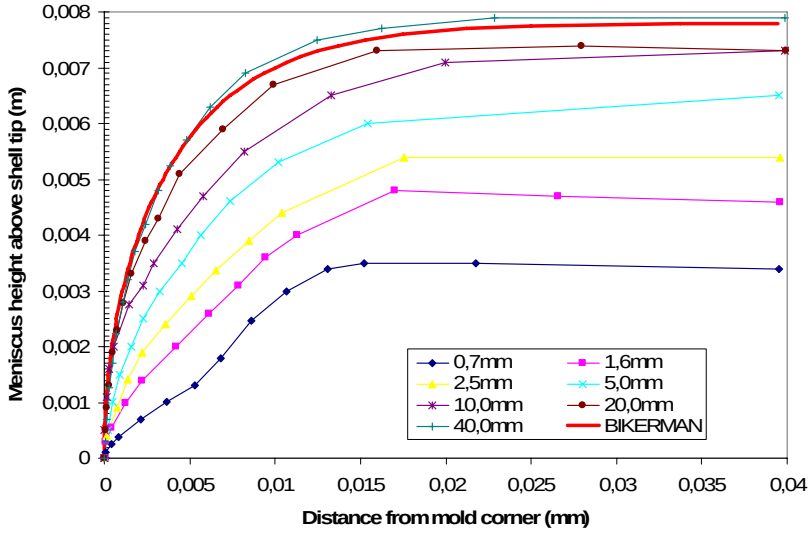

Fig. 8 Sections through the 3-D Interface shape at different distances from mold wall

Steady-state temperature profile

The heat transfer results for the steady-state stagnant (no-flow) 2-D model show the time-averaged temperature distribution in the mold powder, resolidified and liquid flux layers in the meniscus region in Fig. 9. The interface between the liquid and resolidified layers (identified by the 1373K isotherm) curves up to meet the powder layer near the nose of the slag rim. The calculated depth of the liquid slag pool in the region far from the wall is computed to be around 13 mm, which is close to the 15 mm measured using nail-board experiments in the plant by H.J. Shin[34]. The heat flux peak is around 8 mm below the steel level, which is consistent with experimental observations. The shape of the solid rim shown in grey in the fig 9 is also consistent with the shape of slag rims taken from operating continuous casting molds.

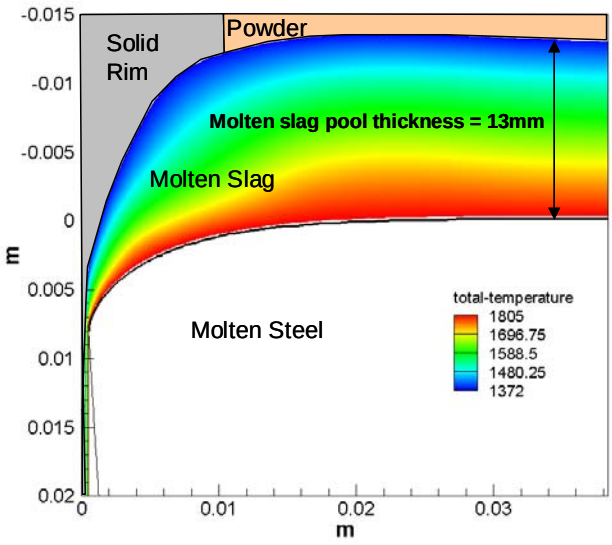

Fig. 9 Heat transfer results (2D model)

Unsteady meniscus shape and flow

After steady state is reached, the events occurring during an oscillation cycle are simulated using the 2-D model. Oscillation is imposed on the mold wall and downward casting velocity is imposed on the shell tip, according to the conditions shown in **table 1**.

Figures. 10-17 show the velocity vectors computed in the meniscus region, colored according to the phase fraction. Red arrows designate slag and blue is the steel phase. The same figures also show the calculated evolution of the shape of the solid slag rim and slag / steel interface with time. Figure 19 summarizes schematically the key events in the flow pattern during the oscillation cycle.

In presenting the results, the oscillation cycle starts arbitrarily at time 0.00 seconds at the beginning of the second cycle in the calculation, when the mold is at its equilibrium position, (matching the far-field metal level) and is moving upward at its maximum speed. The mold reaches its peak height (zero velocity) at 0.097s. Soon after starting downwards, the mold speed exceeds the casting speed, (0.125s) which starts the 0.135s-long "negative strip time" period. Negative strip is needed to prevent sticking of the shell to the mold, which is a relatively rare, but dangerous alternate mechanism of oscillation mark formation. The positive strip time comprises the rest of the oscillation cycle, and starts at 0.261s. The entire cycle ends at the equilibrium position again at 0.387s.

During the first part of the oscillation cycle, when the mold is moving upward, liquid slag flows towards the slag rim to fill the space opened as the rim moves upward, as shown in Fig. 10. Liquid slag is also drawn upward out of the gap between the steel shell and the solid slag layer due to the negative pressure generated by this upwards movement of the mold. This behavior continues until 0.06s. During the positive strip time, the interface between the liquid steel and the liquid slag is pulled towards the mold wall.

At 0.07 s the liquid slag first starts to flow towards the mold wall, as shown in Fig.11. At 0.11 s the molten steel starts to overflow the meniscus and flow into the gap between the solid slag and the solid steel shell. Even after the mold starts downwards (Fig. 12), the momentum of the steel continues to move the interface towards the mold wall.

After the midpoint of negative strip time period, (Fig. 13), the molten steel has completely overflowed the meniscus, finishing at ~0.21s. The downward movement of the slag rim causes a sharp increase in positive pressure. This prediction is qualitatively consistent with the mechanism of Sengupta[1], and with the computations of Takeuchi [5]. The pressure starts to push molten slag out of the region between the solid slag rim and the interface in both directions: into the shell / mold gap (where it provides lubrication consumption)

and towards the center of the mold. The new slag / steel interface, which is established after the overflow, is pushed further away from the mold wall.

During the negative strip time, liquid slag is pushed into the gap, which increases the consumption rate of liquid slag as shown in Fig. 20. However, the movement of the solid slag rim downwards creates a force against the interface between the liquid steel and the liquid slag. This pushes the slag out of the meniscus region at relatively high velocity (Fig. 17). This flow pattern continues during the negative strip period and the downward movement of the mold until 0.29s. The interface shape continues to move away from the mold wall during the downward movement of the mold, except for the overflowed steel that remains in the shell / mold gap and would solidify.

During the upward movement of the mold, (Fig. 17), the results show again that the liquid slag is flowing out of the gap between the solid slag and solid steel shell and the direction of the flow in the meniscus region under the solid slag rim is towards this solid rim. The pressure during this period decreases and the flow pattern changes and goes against the solid rim into the meniscus region. During this period the interface starts to move toward the mold wall again. At the end of the oscillation cycle, the results are almost the same as the results at 0.01s, which shows that the model is at pseudo-steady state: at the same point in the oscillation curve, the same results are predicted.

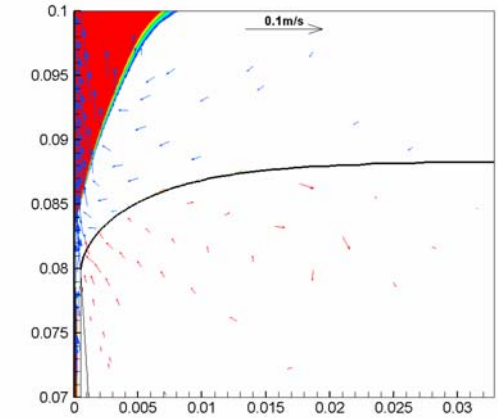

Fig. 10 Rim shape, interface shape and velocity vectors at 0.01s

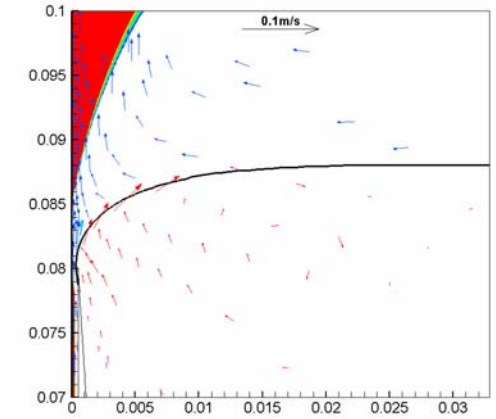

Fig. 11 Rim shape, interface shape and velocity vectors at 0.06s

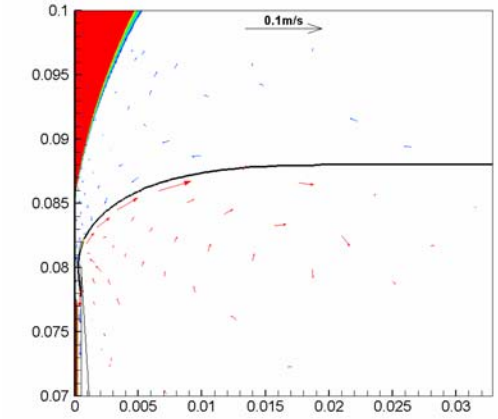

Fig. 12 Rim shape, interface shape and velocity vectors at 0.10s

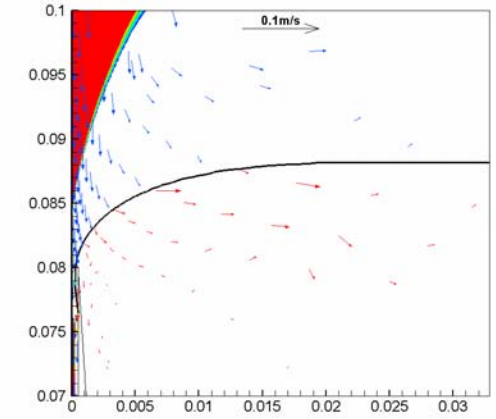

Fig. 13 Rim shape, interface shape and velocity vectors at 0.14s

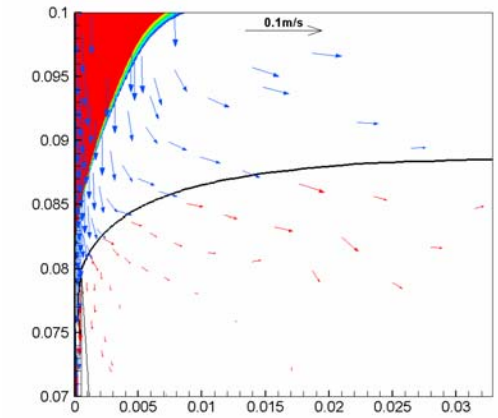

Fig. 14 Rim shape, interface shape and velocity vectors at 0.19s

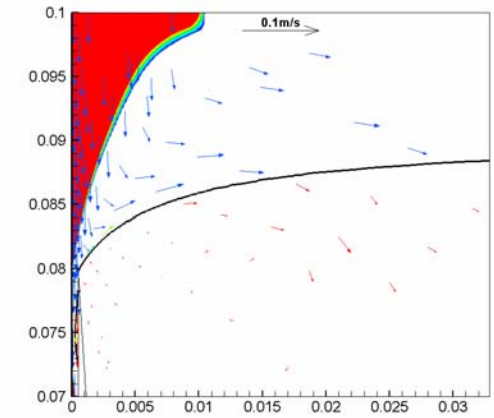

Fig. 15 Rim shape, interface shape and velocity vectors at 0.24s

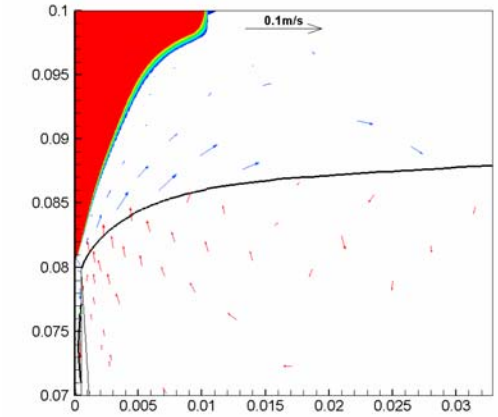

Fig. 16 Rim shape, interface shape and velocity vectors at 0.29s

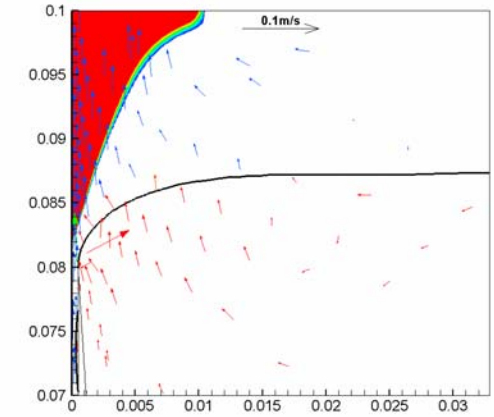

Fig. 17 Rim shape, interface shape and velocity vectors at 0.34s

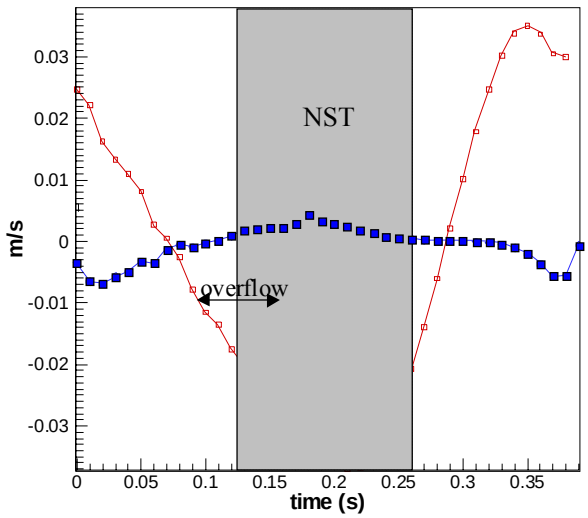

Fig. 18 Vertical component at the gap entrance (circles) and horizontal component far from gap (filled squares) of the velocity

Summary of meniscus flow events

As shown schematically in Fig.19, during the positive strip time (until 0.09s), upward movement of the slag rim opens up the space above the meniscus and draws in liquid slag. Slag consumption into the gap between the steel shell and the mold is negative, and the meniscus is pulled towards the mold. Just before negative strip starts, the meniscus overflows the top of the shell. After this point, there is positive slag consumption into the gap (see Fig. 20). During the negative strip time, downward mold movement generates positive pressure and squeezes slag out of the shrinking meniscus region. Also during this period, the overflowed steel solidifies in the mold / shell gap, while a new meniscus forms and is pushed away from the mold. As the positive strip period begins again, the pressure decreases and the slag again flows beneath the rim and pulls the interface towards the mold.

Upward vertical (y) velocity near the gap inlet increases greatly during the positive strip time, as shown in Fig. 18. This prediction agrees with experimental observations by Tsutsumi et al.[5, 26] At the same time, horizontal (x) velocity at a point far from the gap is towards the slag rim, (negative), as slag flows into the meniscus region. Later, during negative strip, horizontal velocity at this point reverses, illustrating how fast the liquid slag is squeezed out.

The flow model predicts that meniscus overflow starts at ~ 2/6 of the oscillation cycle before the start of the negative strip time. Running the model for more than one oscillation cycle again predicts an overflow event at the same time as in the previous oscillation. Starting the simulation case from a different point in the oscillation cycle (the time of maximum downstroke velocity) delayed the overflow event to later during the negative strip time and continuing during the positive strip. Continuing this case for another cycle, the second overflow event starts at ~2/6 of the oscillation curve before negative strip, as before. These results suggest that although the overflow event is consistent for a given set of conditions, minor changes, such as caused by level fluctuations or a different flux rim shape, can make overflow occur at a different time in the cycle.

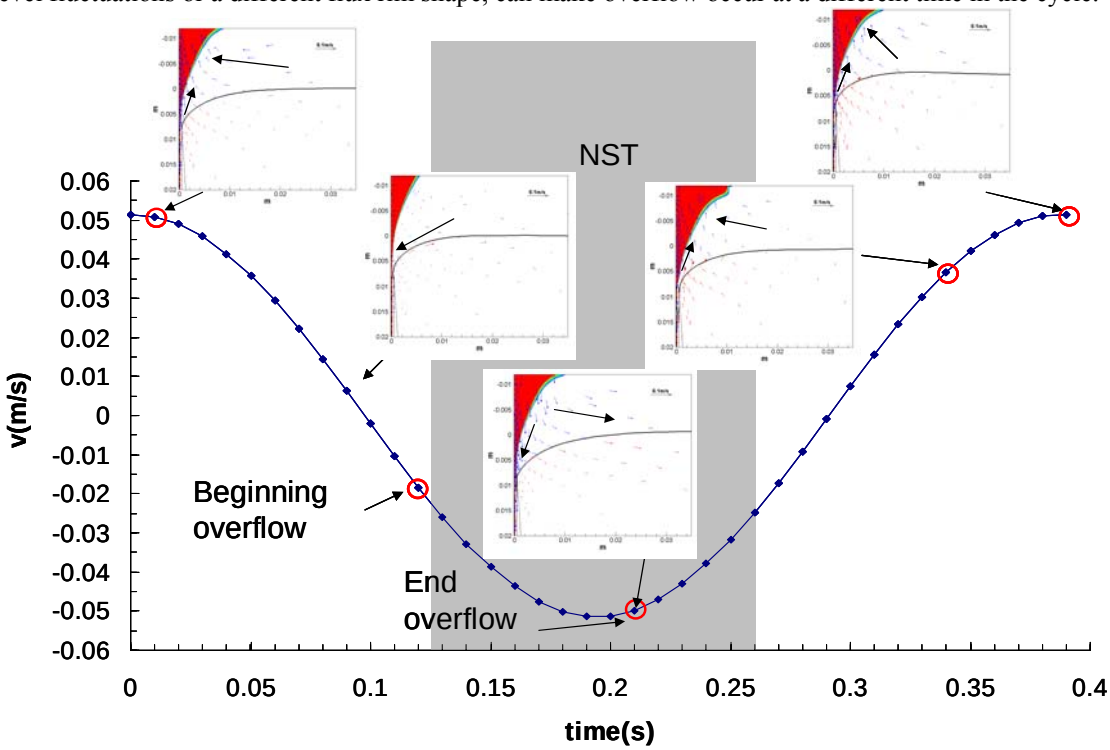

Fig. 19 Scheme of the evolution of the floor and interface shape during one oscillation cycle

Slag Consumption

The instantaneous and mean consumption rate of liquid slag into the gap between the solid steel shell and the mold are shown in Fig. 20. Positive consumption starts when the overflow event drives both liquid slag and molten steel into the gap, where it is captured within the newly-formed oscillation mark. Positive consumption continues during the negative strip time, as pressure from the downward movement of the slag rim pushes slag into the gap. Positive consumption continues into the positive strip period until 0.32s, as

shear stress from the downward moving steel shell drags in the liquid slag. Negative consumption (slag leaving the gap) occurs only during that part of the positive strip time that the mold is moving upwards near its maximum velocity.

The net result is that there is a positive mean consumption into the gap of 0.0061 kg/ms, (2.36 g/m/cycle) which is close to the consumption rate of 0.0058kg/ms (2.25 g/m/cycle) measured in the steel caster for the same operational data by Shin et al.[26,34]. The overflow event has only a minor effect on distorting the consumption curve, which is otherwise a sinusoidal curve consistent with previous work[5,26].

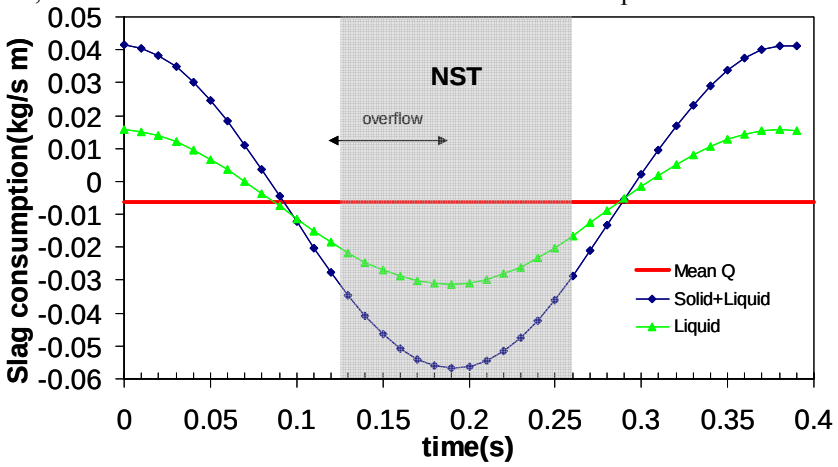

Fig. 20 Consumption of slag into the gap during one oscillation cycle

Unsteady Heat transfer

The model results were further analyzed to determine the heat flux to the solidified flux layer on the left side of the domain, which then enters the water-cooled mold wall. The heat flux can be decomposed into a variable component and a mean component[35]. In this case the average component calculated by the model is around 2.7 MW/m^2. The profile, given in Fig. 21, shows the evolution of the variable component of the heat flux at a point located in the mold at the shell tip height ~8mm below the free surface. It is clearly shown that due to the overflow event, there is a sudden increase in the heat flux at this point. After this time, there is a decrease in the heat flow, due to the separation of the interface from the wall. From the perspective a point moving with the oscillating mold, the heat flux appears to increase almost continuously through the negative strip period, which is consistent with measurements made by Badri and coworkers[35]. In this model, the effect of the latent heat delivered by the solidification of the steel is not taken into account. This would further increase heat flow, making the match with experimental observations even better.

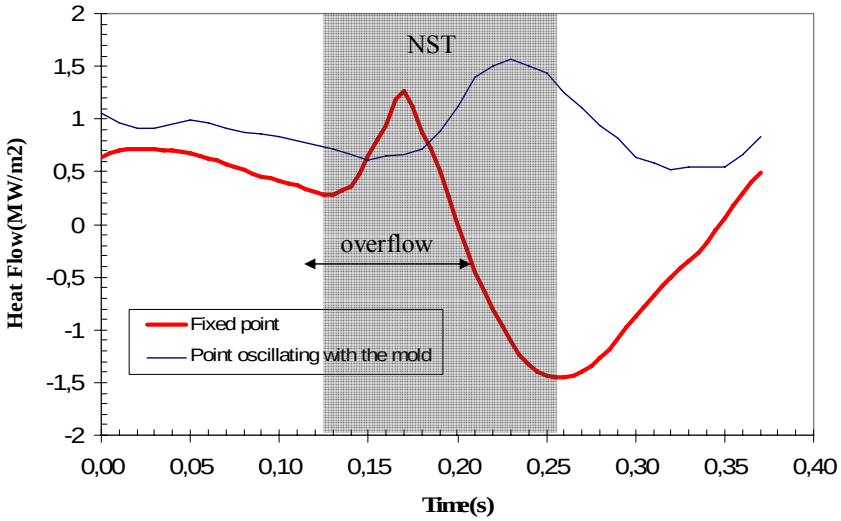

Fig. 21 Heat flux evolution at the shell tip during one oscillation cycle

Mechanism of hook formation and shape

These model results give new insight into the mechanism for hook and oscillation mark formation, and reconcile previous measurements with theory. Alternating pressure due to mold oscillation and interaction with the solidified flux rim causes meniscus motion, and overflow just before the negative strip time starts, although the results suggest that overflow could happen at various times during the oscillation cycle. If the molten steel in the region becomes supercooled, the meniscus could solidify at some time during the cycle before overflow, leading to hook formation. Thus, the different shapes of the interface (meniscus) predicted at different times in the cycle are compared in Fig. 22 with hook shapes measured in samples from a real caster.[5, 26] The predicted range agrees remarkably well with the measurements. The curvatures also agree well, although there appears to be slightly more curvature in the measured hooks. This suggests that other phenomena, such as level fluctuations or thermal distortion may have altered the hook shape.[1] Thermal distortion is the most likely explanation, however, as the heating provided from the molten steel to the outside of the hook during overflow would cause it to expand and distort, increasing its curvature from the predicted shape of the meniscus to that observed in the solidified hook.

In fig. 22 is shown the evolution of the interface shape for a cut starting in the corner keeping 45º between the faces. The lines with symbols are the results taken from the model and the ones without symbols are the ones taken from the measurements made by G. Lee and coworkers [36]. The interface shape movement predicted by the model agrees very well with the measurements, especially at its highest position (time=0.10s) when the meniscus freezing is more likely to happen because the interface is closer to the wall and the heat flux higher.

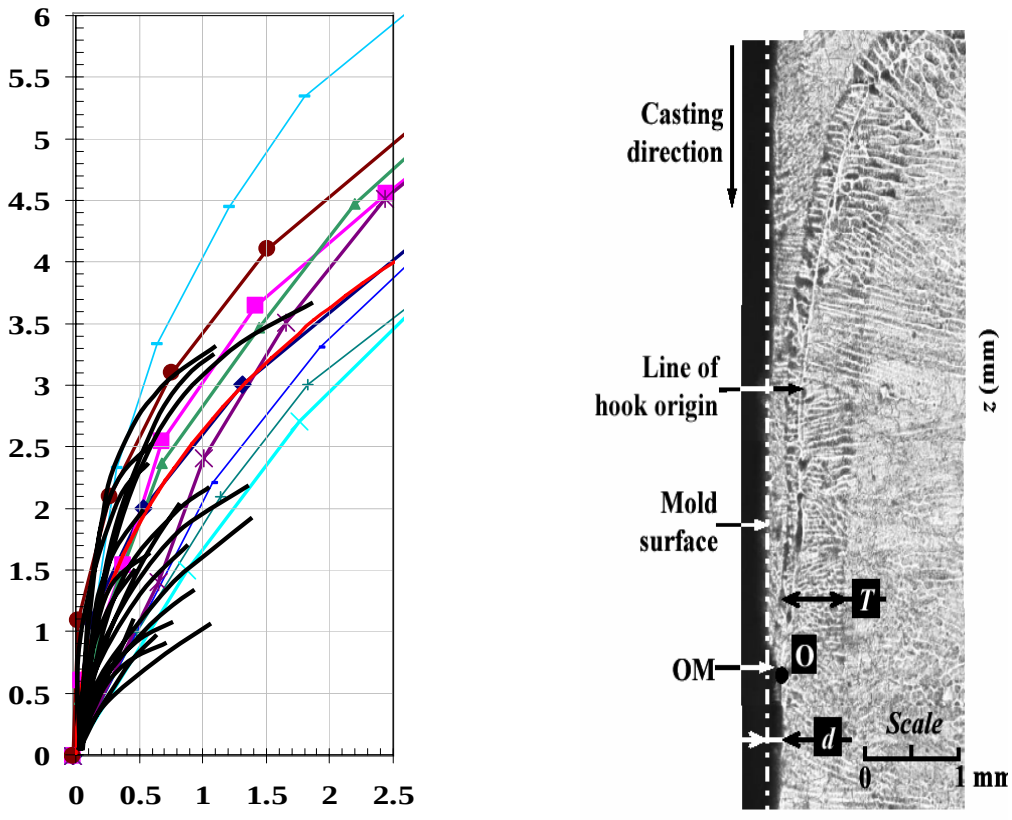

Fig. 22 Evolution of the interface shape comparing with measurements [1, 34]

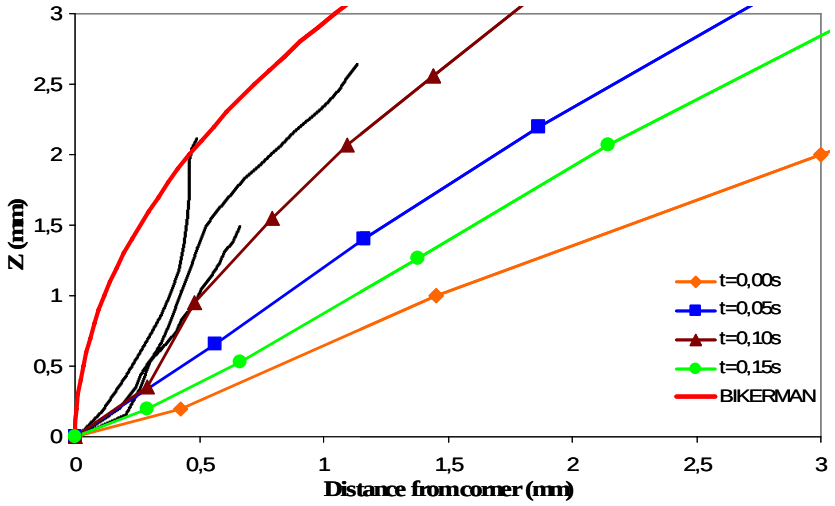

Fig. 23 Comparison of the Interface shape evolution with time (symbols lines) and measurements [36] (lines without symbols)

CONCLUSIONS

A transient computational model of fluid flow and heat transfer in the meniscus region has been developed, validated with measurements, and applied to gain new insights into oscillation phenomena:

- The oscillating solidified slag rim controls the flow pattern in the meniscus region.
- Pressure in the gap between the shell and mold oscillates between positive pressure (compression) during negative strip and negative pressure (vacuum) during positive strip..
- Computations and experimental data both show that the overflow event can start at different times during the oscillation cycle, but often starts ~beginning of negative strip time.
- Overflow starts earlier with a more severe solid slag rim.
- Liquid flux consumption varies continuously during the oscillation cycle, but is consumed into the gap only during negative strip time.
- The heat flux peak occurs ~1 cm below the meniscus level, owing to meniscus curvature.
- The range of meniscus shapes predicted during the oscillation cycle matches well with the range of shapes of measured hooks.
- The slight extra curvature appearing in hook measurements might be due to thermal strain and requires further study.
- The meniscus sometimes drops below the shell tip, exposing it to slag, and creating relatively straight hooks with associated surface defects. This is expected to be more likely with a more severe solid slag rim or level fluctuations.

ACKNOWLEDGEMENTS

The authors are grateful to Fundacion Labein – Tecnalia, Derio, Spain, the National Science Foundation (Grant DMI 04-23794), and the Continuous Casting Consortium at University of Illinois at Urbana-Champaign for support of this project, and to Fluent Inc., for supplying the FLUENT package. They also want to thank Go Gi Lee for providing and helping with the interpretation of the experimental data.

REFERENCES

1. J. Sengupta, B.G. Thomas, H.-J. Shin, G.-G. Lee and S.-H. Kim, *"A new mechanism of hook formation during continuous casting of ultra-low carbon steel slabs,"* Metallurgical and materials transactions A, 2005.
2. B.G.Thomas, *"Slab casting phenomena,"* 2005, Continuous Casting Consortium Website.

3. H. Steinruck and C. Rudischer, *"Numerical investigation of the entrainment of flux into the lubrication gap in continuous casting of steel*," in *Fifth World Congress on Computational Mechanics*. 2002. Viena, Austria.
4. J.R. King, A.A. Lacey, C.P. Please, P. Wilmott and A. Zoryk, *"The formation of oscillation marks on continuously cast steel,"* Math. Engng. Ind., 1993. 4(2): p. 91-106.
5. E. Takeuchi and J.K. Brimacombe, *"The formation of oscillation marks in the continuous casting of steel slabs,"* Metallurgical Transactions B, 1984. 15B: p. 493-509.
6. C. Perrot, J.N. Pontoire, C. Marchionni, M.R. Ridolfi and L.F. Sancho, *"Several slag rims and lubrication behaviors in slab castings,"* in *European Continuous Casting Conference 2005*. 2005.
7. S. Takeuchi, Y. Miki, S. Itoyama, K. Kobayashi, K.-I. Sorimachi and T. Sakuraya, *"Control of oscillation mark formation during continuous casting,"* in *Steelmaking conference proceedings*. 1991.
8. R.B. Mahapatra, J.K. Brimacombe and I.V. Samarasekera, *"Mold behavior and its influence on quality in the continuous casting of steel slabs: Part II. Mold heat transfer, mold flux behavior, formation of oscillation marks, longitudinal off-corner depressions, and subsurface cracks,"* Metallurgical Transactions B, 1991. 22B: p. 875-888.
9. I.V. Samarasekera, *"Crack formation,"* in *Brimacombe Continuous Casting Course*, 2005. p. Secction R.
10. E. Takeuchi and J.K. Brimacombe M. Hanao, M. Kawamoto, T. Murakami and H. Kikuchi, *"Effect of oscillation-mark formation on the surf ace quality of continuously cast steel slabs,"* Metallurgical Transactions B, 1985. 16B: p. 605-625.
11. Y. Meng, B.G. Thomas, A.A. Polycarpou, H. Henein and A. Prasad. *"Mold slag measurements to characterize CC mold-shell gap phenomena,"* in *Materials Science & Technology 2004*. 2004. New Orleans, LA.
12. Y. Meng and B.G. Thomas, *"Heat transfer and solidification model of continuous slab casting: CON1D,"* Metallurgical Transactions B, 2003. 34B: p. 685-705.
13. M. Hanao, M. Kawamoto, T. Murakami and H. Kikuchi, *"Mold flux for high speed continuous casting of hypoperitectic steel slabs,"* in *European Continuous Casting Conference 2005*. 2005.
14. K.C. Mills and A. B. Fox, "*The role of mould fluxes in continuous casting-So simple yet so complex,"* ISIJ International, 2003. 43(10): p. 1479-1486.
15. S. McKay, N.S. Hunter, A.S. Normanton, V. Ludlow, P.N. Hewitt and B. Harris, *"Continuous casting mould powder evaluation,"* Ironmaking and Steelmaking, 2002. 29(3): p. 185-190.
16. K.C. Mills, A. B. Fox, and M.C. Bezerra, *"A logical approach to mould powder selection,"* in *MMT 2000*. 2000.
17. K.Schwerdtfeger and H. Sha, *Depth of oscillation marks forming in continuous casting of steel.* Metallurgical and Materials Transactions B, 2000. **31B**: p. 813-826.
18 H. Steinruck, C.Rudischer and W.Schneider, "*The formation of oscillation marks in continuous casting of steel*." in *Modeling of Casting, Welding and Advanced Solidification Processes VIII*. 1998: The Minerals, Metals and Materials Society.
19 Thomas, B.G. and H. Zhu, Thermal Distortion of Solidifying Shell in Continuous Casting of Steel, in Proceedings of Internat. Symposia on Advanced Materials & Tech. for 21st Century, I. Ohnaka and D. Stefanescu, Editors. 1996, TMS, Warrendale, PA: Honolulu, HI. p. 197-208.20 J. Barco, M. Ojanguren, J. Palacios, M. Serna, C. Ojeda and V. Santisteban, *"Global modelization of continuous casting process,"* in European Continuous Casting Conference, 2005. Nize.
21. B.G. Thomas and F.M. Najjar, *"Finite element modelling of turbulent fluid flow and heat transfer in continuous casting,"* Applied Mathematical Modeling, 1991. 15: p. 226-243.
22. Y. Meng and B.G. Thomas, *"Modeling transient slag layer phenomena in the shell/mold gap in continuous casting of steel,"* Metallurgical and materials transactions B, 2003. 34B: p. 707-725.
23. R.M. McDavid and B.G. Thomas, *"Flow and thermal behavior on the top surface flux/powder layers in continuous casting molds,"* Metallurgical and materials transactions B, 1996. 27B: p. 672-685.
24. C.A. Pinheiro, I.V. Samarasekera and J.K. Brimacombe, *"Mold flux for continuous casting of steel,"* in *I&SM*. 1994 - 1995 - 1996.
25. J. Sengupta and B.G. Thomas, *"Visualization of hook and oscillation mark formation mechanism in ultra-low carbon steel slabs during continuous casting,"* JOM-e(TMS), 2005: p. 1-21.
26. E. Anzai, T. Ando, T. Shigezumi, M. Ikeda and T. Nakano, *"Hydrodynamic behavior of molten powder in meniscus zone of continuous casting mold,"* 1987, Nippon Steel. p. 31-40.
27. J. Sengupta, H.-J. Shin., B.G. Thomas and S.-H. Kim, "Micrograph evidence of meniscus solidification and sub-surface microstructure evolution in continuous-cast ultra-low carbon steels," Acta Materiala, 2005.

28. H.-J. Shin, G.-G.Lee., S.-M. Kang, S.-H. Kim, W.-Y. Choi, J.-H. Park, and B.G. Thomas, "*Effect of mold oscillation on powder consumption and hook formation in ultralow-carbon steel slabs,"* Iron and Steel Technology, 2005: p. 56-69.
29. .K. Tsutsumi, J.-I. Ohtake and M. Hino, *"Inflow behavior observation of molten mold powder between mold and solidified shell by continuous casting simulator using Sn-Pb alloy and stearic acid,"* ISIJ International, 2000. 40(6): p. 601-608.
30. B. Zhao, S.P. Vanka and B.G. Thomas, *"Numerical study of flow and heat transfer in a molten flux layer,"* International Journal of Heat and Fluid Flow, 2005. 26: p. 105-118.
31. S. Furuhashi, M. Yoshida, and T. Tanaka: *Tetsu-to-Hagane*, **84** (1998), pp. 625-631.
32. C. Ojeda, J. Sengupta, J. Barco, J.L. Arana and B.G. Thomas: Mathematical modeling of thermal-fluid flow in the meniscus region during an oscillation cycle; AISTech 2006, May 1-4 2006.
33. J. Sengupta and B.G. Thomas, "Modeling of Casting, Welding and Advanced Solidification Processes XI", 2006
34. H.J. Shin, PhD Thesis, 2006
35. A.Badri, T.T.Natarajan, C.C.Snyder, K.D.Powders, F.J.Mannion and A.W.Cramb, Met. and Mat. Trans. B, 2005
36. G. Lee, , HJ Shin, BG Thomas, and SH Kim, "Three-dimensional microstructure of frozen meniscus and hooks in continuous-cast ultra-low-carbon steel slabs", AISTech 2007, Indianapolis, IN, April, 2007, AIST.